Amino Acids (2015) 47:1155–1166
DOI 10.1007/s00726-015-1943-z

ORIGINAL ARTICLE

New insights into novel inhibitors against deoxyhypusine hydroxylase from plasmodium falciparum: compounds with an iron chelating potential

Imke von Koschitzky · Heike Gerhardt · Michael Lämmerhofer · Michal Kohout · Matthias Gehringer · Stefan Laufer · Mario Pink · Simone Schmitz-Spanke · Christina Strube · Annette Kaiser

Received: 17 December 2014 / Accepted: 14 February 2015 / Published online: 26 February 2015

Abstract Deoxyhypusine hydroxylase (DOHH) is a dinuclear iron enzyme required for hydroxylation of the aminobutyl side chain of deoxyhypusine in eukaryotic translation initiation factor 5A (eIF-5A), the second step in hypusine biosynthesis. DOHH has been recently identified in *P. falciparum* and *P. vivax*. Both enzymes have very peculiar features including E–Z type HEAT-like repeats and a diiron centre in their active site. Both proteins share only 26 % amino acid identity to the human paralogue. Hitherto, no X-ray structure exists from either enzyme. However, structural predictions based on the amino acid sequence of the active site in comparison to the human enzyme show that four conserved histidine and glutamate residues provide the coordination sites for chelating the ferrous iron ions. Recently, we showed that *P. vivax* DOHH is inhibited by zileuton (*N*-[1-(1-benzothien-2-yl)ethyl]-*N*-hydroxyurea), a drug that is known for inhibiting human 5-lipoygenase (5-LOX) by the complexation of ferrous iron. A novel discovery program was launched to identify inhibitors of the *P. falciparum* DOHH from the Malaria Box, consisting of 400 chemical compounds, which are highly active in the erythrocytic stages of Malaria infections. In a first visual selection for potential ligands of ferrous iron, three compounds from different scaffold classes namely the diazonapthyl benzimidazole MMV666023 (Malaria Box plate A, position A03), the bis-benzimidazole MMV007384 (plate A, position B08), and a 1,2,5,-oxadiazole MMV665805 (plate A, position C03) were selected and subsequently evaluated in silico for their potential to complex iron ions. As a proof of principle, a bioanalytical assay was performed and the inhibition of hypusine biosynthesis was determined by GC–MS. All tested compounds proved to be active in this assay and MMV665805 exhibited the strongest inhibitory effect. Notably, the results were in accordance with the preliminary

Handling Editor: Michael Platten

I. von Koschitzky and H. Gerhardt share the first authorship.

I. von Koschitzky · A. Kaiser
Institute for Pharmacogenetics, Medical Research Centre, University Duisburg-Essen, Hufelandstrasse 55, 45147 Essen, Germany

H. Gerhardt · M. Lämmerhofer
Institute of Pharmaceutical Sciences, Pharmaceutical (Bio) Analysis, Eberhard-Karls-University Tübingen, Auf der Morgenstelle 8, 72076 Tübingen, Germany

M. Kohout
Department of Organic Chemistry, Institute of Chemical Technology Prague, Technická 5, 166 28 Prague, Czech Republic

M. Gehringer · S. Laufer
Pharmaceutical and Medicinal Chemistry, Institute of Pharmaceutical Sciences, Eberhard-Karls-University Tübingen, Auf der Morgenstelle 8, 72076 Tübingen, Germany

M. Pink · S. Schmitz-Spanke
Institute and Outpatient Clinic of Occupational, Social and Environmental Medicine, University of Erlangen-Nürnberg, Schillerstrasse 25/29, 91054 Erlangen, Germany

C. Strube
Institute for Parasitology, University of Veterinary Medicine Hannover, Bünteweg 17, 30559 Hannover, Germany

Present Address:
A. Kaiser (✉)
Fraunhofer Institut IME, Forckenbeck Strasse 6, 52074 Aachen, Germany
e-mail: annette.kaiser@ime.fraunhofer.de

quantum–mechanical calculations suggesting the strongest iron complexation capacity for MMV665805. This compound might be a useful tool as well as a novel lead structure for inhibitors of *P. falciparum* DOHH.

Keywords Deoxyhypusine hydroxylase · Hypusine · Plasmodium · Malaria Box · Iron chelators

Introduction

During recent years, it has been shown that biosynthetic enzymes of the polyamine pathway are important drug targets. Ornithine decarboxylase combats African sleeping sickness (Milord et al. 1992) emphasizing its importance in hyperproliferating parasite cells. Most notably, unbound polyamines constitute 14 % of the parasite's metabolome (Teng et al. 2009). However, the enucleated human erythrocyte does not possess biosynthetic enzymes for active polyamine biosynthesis resulting in low polyamine concentrations in the range of 5–50 µM. During malaria infection, there is notable rise in polyamine levels during the trophozoite to schizont stage transition (Birkholtz et al. 2011). In correlation with the increase of polyamine levels, the activity of regulatory key enzymes, i.e., *S*-adenosylmethionine-decarboxylase (SAMDC) and spermidine synthase (SPSYS) is elevated during schizogeny (Assaraf et al. 1984).

The unusual amino acid hypusine is formed by post-translational modification of a lysine side chain (K 51 in human) in eukaryotic translation initiation factor 5A (eIF-5A) (Kaiser 2012). Biosynthesis of hypusine (Fig. 1) comprises two enzymatic steps. The first step is the transfer of an aminobutyl moiety from the polyamine spermidine to the ε-amino group of a specific lysine in eIF-5A, which is catalyzed by deoxyhypusine synthase (DHS, EC 2.5.1.46) (Umland et al. 2004). In the second step, deoxyhypusine hydroxylase (DOHH, EC 1.14.99.29) (Park et al. 2006) completes hypusine biosynthesis by hydroxylation of the side chain and thus activates eIF-5A. Both enzymes have been first identified from human and yeast (Thompson et al. 2003) and subsequently in other eukaryotes but hitherto not in archae.

Out of the last mentioned enzymes, DOHH is more interesting as a potential target for drug discovery because of its distinct structural features. Structural analyses based on homology models revealed a HEAT-repeat-containing protein with eight tandem repeats of an α-helical pair organized in a symmetrical dyad (Park et al. 2006). These HEAT-repeat like structures suggest an interaction with different proteins. However, disrupting protein–protein interactions by small molecules has proved to be a challenging task. Notwithstanding, an iron-complexing

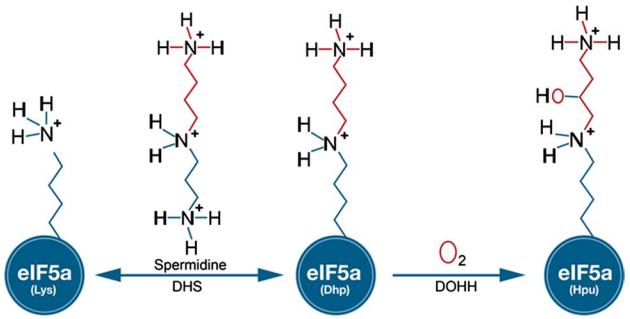

Fig. 1 Biosynthetic pathway leading to hypusine modified eIF-5A. Hypusine biosynthesis is performed within two consecutive steps catalyzed by deoxyhypusine synthase (DHS) transferring the aminobutyl moiety from spermidine to a specific lysine (lysine 51) residue in eIF-5A. In a second step the hydroxyl group is introduced to the aminobutyl moiety by deoxyhypusine hydroxylase (DOHH)

strategy seemed promising since DOHH has four histidine–glutamate residue pairs, which coordinate ferrous iron. Moreover, human DOHH has an oxygen regulated diiron centre, which forms a blue chromophore based on a (-1,2-peroxo)diiron(III)) complex upon the reaction of the reduced enzyme with O_2 (Vu et al. 2009). The DOHH structure is unrelated to beta-helix type structures of the Fe(II)- and 2-oxoacid-dependent dioxygenases like collagen prolyl- and lysine lyases (Park et al. 2006). Furthermore, DOHH is essential for proliferation in the budding yeast but not in the fission yeast (Kang et al. 2007). The mechanism of iron regulation has been recently studied for human DOHH (Frey et al. 2014). Two iron chaperons, PCBP1 and PCBP2 (polyrC binding proteins) known to bind iron and deliver it to ferritin and prolylhydroxylases are involved in the transfer of the ferrous iron to the metalloprotein DOHH (Frey et al. 2014).

Hitherto, parasitic DOHH has only been identified in different *Plasmodium* species, i.e., *P. falciparum* (Frommholz et al. 2009) and *P. vivax* (Atemnkeng et al. 2013) and recently in *Leishmania donovani* (Chawla et al. 2012). The enzymes share common structural elements like the aforementioned EZ-HEAT-like repeat motifs are also present in E/F type phycocyanin lyases from cyanobacteria. However, the number of HEAT-like repeats differs between the two *Plasmodium* species. While five HEAT-repeats occur in *P. falciparum* DOHH, only four are present in *P. vivax,* similar to the human paralogue. Both DOHH proteins from *P. vivax* and *P. falciparum* contain a highly conserved histidine–glutamate (HE)-motif coordinating the ferrous iron. Despite the fact that both proteins have structural features in common with the human paralogue, they share only 26 % amino acid identity with the human counterpart.

To date, the human DOHH has only been targeted with small iron chelating molecules, which inhibited the enzyme with a widely varying efficacy (Andrus et al. 1998; Clement

et al. 2002). Among the molecules tested, the inhibitory activity decreases in the following order: ciclopirox> deferoxamine> 2,2′-dipyridyl> deferiprone> mimosine ($IC_{(50)}$ range: 5–200 µM). Moreover, these compounds inhibited recombinant DOHH from *P. falciparum* and *P. vivax* in vitro. However, a translational approach in a rodent model infected with the *P. berghei* ANKA strain caused death of the mice since the drugs obviously chelated additional metalloproteins (Saeftel et al. 2006). These results emphasize the necessity for inhibitors, which are highly selective for the plasmodial enzyme and effective in vivo without affecting the human paralogue. DOHH from *P. vivax* has already been evaluated (Atemnkeng et al. 2013) since this parasite causes severe clinical symptoms and a relapse due to dormant hypnozoites after a primary infection has been cleared. The dormant hypnozoites persist in the hepatocytes of the liver. Primaquine is the only drug affecting the hypnozoites (Krotoski 1989) but it cannot be administered in case of pregnancy and patients with glucose-6-phosphate dehydrogenase deficiency, which occurs in malaria-endemic regions (Baird and Hoffman 2004). In the present study, we focus on DOHH from *P. falciparum* which differs in the number of EZ-HEAT repeats with respect to the human counterpart.

To discover novel antimalarials selectively chelating the ferrous iron of DOHH from *Plasmodium falciparum* we screened the Malaria Box (Spangenberg et al. 2013; von Koschitzky and Kaiser 2013), an open access compound set from different resources, i.e., GlaxoSmith Kline (GSK), the Tres Cantos Antimalarial Set, the Novartis-GNF Malaria Box Data set and St. Jude Children's Research Hospital (Guiguemde et al. 2010). In a first phenotypic forward chemical genetic approach, the 400 compounds from the Malaria Box were tested for their ability to eradicate the parasite in the erythrocytic stages. More than 10 % of the compounds exhibited antiplasmodial activity in the nanomolar range against the chloroquine resistant *P. falciparum* 3D7 strain. These compounds were preselected and subdivided into drug-like and molecular probe-like molecules in the Malaria Box. Forty active compounds with an IC_{50} < 2 µM were selected because they eradicated the parasite in the blood stages. As obvious from visual inspection, the majority of those compounds could either function as metal chelators or act as kinase inhibitors, depending on their particular scaffolds. Three potential ligands of ferrous iron located on the Malaria Box microtiter plate A, i.e., the benzimidazole inhibitors, position A03, MMV666023 and position B08, MMV007384, and a 1,2,5-oxadiazole (position C03) MMV665805 were identified and are depicted in Fig. 2.

The three identified compounds showed different EC_{50} values in the range between 36.8 nM (MMV666023), 177 nM (MMV007384) and 117 nM (MMV665805) when tested in a *P. falciparum* in vitro culture (Gamo et al. 2010). After addition of 2 µM of each compound, the rate of inhibition in the hypusine assay was 96 % for MMV666023, 98 % for MMV007384 and 97 % for MMV665805. These inhibitors were further analyzed for their capacity to inhibit *P. falciparum* DOHH in a target-based screen.

Materials and methods

Enzymatic synthesis of hypusine

In order to perform a *P. falciparum* enzyme activity assay, both purified modified *P. vivax* eIF-5A$^{(dhp)}$ and purified *P. falciparum* DOHH are necessary. To facilitate the first step of eIF-5A modification, purified recombinant eIF-5A from *P. vivax* was modified with recombinant human DHS, which has low substrate affinity but higher specific enzyme activity than the parasitic enzyme (Kaiser et al. 2007), and achieves the same modification. Both human DHS and *P. vivax* eIF-5A were *N*-terminally histidine tagged fusion proteins in recombinant *pET-15b* vectors and successfully expressed in *E. coli* BL21. After cell lysis, purification by Nickel-chelate affinity chromatography under native conditions was performed. Subsequently, a buffer exchange with

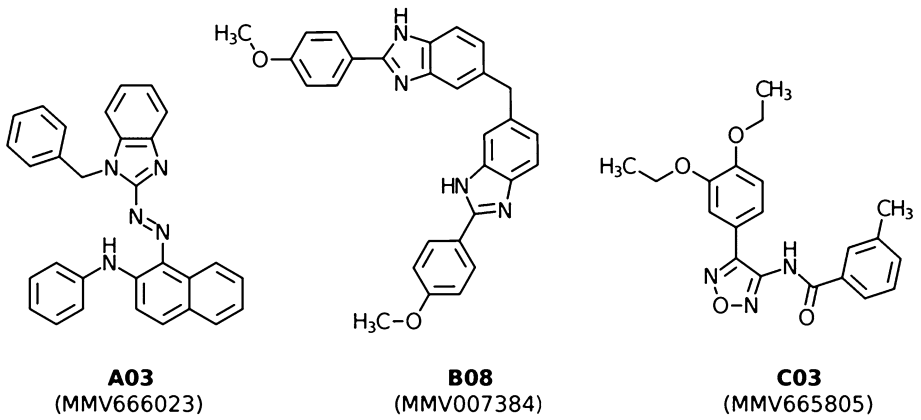

Fig. 2 Identified potential iron chelators in the Malaria Box. 1. *A03 MMV666023 N*-phenyl-1-[1-(phenylmethyl)benzimidazol-2-yl]diazenylnaphthalen-2-amine, 2. *B08 MMV007384* [2-(4-methoxyphenyl)-6-[[2-(4-methoxyphenyl)-3*H*-benzimidazol-5-yl]methyl]-1H-benzimidazole] 3. *C03 MMV665805 N*-[4-(3,4-diethoxyphenyl)-1,2,5-oxadiazole-3-yl]-3-methylbenzamide]

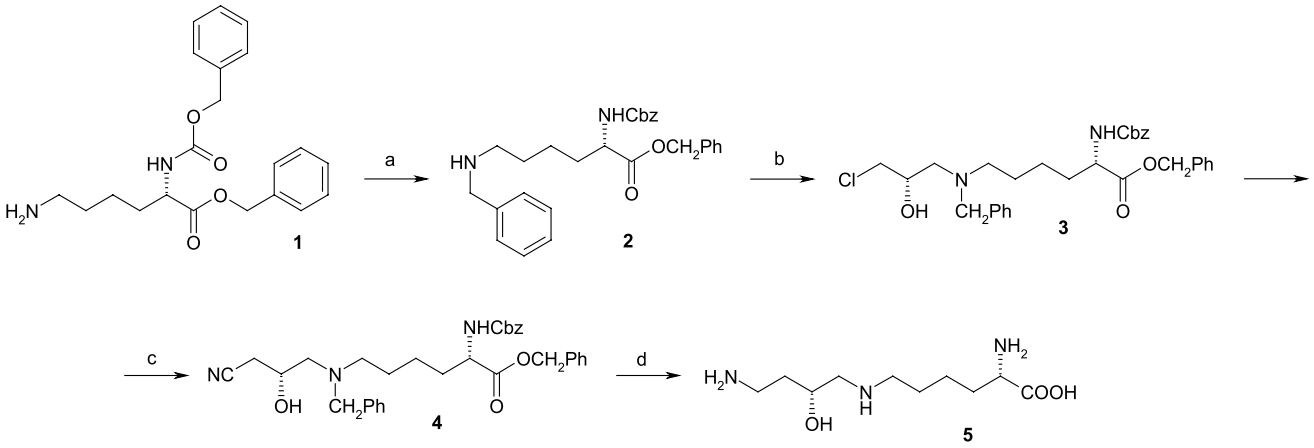

Fig. 3 Synthesis of (2*S*, 9*R*)-hypusine, **a** benzaldehyde, $NaBH_3CN$; **b** (*S*)-(+)-epichlorohydrin; **c** KCN, 18-crown-6, acetonitrile, reflux; **d** H2/PtO2, 0.1 MPa, CH3COOH. *N*-Cbz-L-lysine benzyl ester phenylsulfonate was obtained from Bachem AG (Bubendorf, Switzerland), (*S*)-(+)-epichlorhydrin and other reagents were purchased from Sigma-Aldrich (Prague, Czech Republic)

0.1 M glycine/NaOH buffer was carried out. The enzyme activity assay was performed in a total volume of 1 ml, containing of 25 µg human DHS, 40 µg purified *P. vivax* eIF-5A precursor protein, 4 mM spermidine, 3 mM NAD, 147 µl protease inhibitor cocktail (Roche, Mannheim, Germany) and 0.1 M glycine NaOH buffer. Incubation took place at 37 °C in a shaker overnight and was stopped by freezing at −80 °C. Following incubation, a two-step size exclusion chromatography with Amicon-Ultracel filters (Amicon, Schwalbach, Germany) of 30 kDa and 100 kDa pore size (Frommholz et al. 2009) was performed to remove the human DHS and concentrate the modified eIF-5A $^{(dhp)}$ for further use.

Cloning of the *dohh* gene into the expression vector p*ET-28a* and its expression in *E. coli* BL21 cells was described previously (Frommholz et al. 2009). Following Nickel-chelate affinity chromatography and rebuffering with 50 mM NaH_2PO_4 buffer, the protein concentration was determined and the purified DOHH protein was used in the enzyme activity assay. 600 µl of enzyme activity assay solution contained 7.5 µg purified *P. falciparum* DOHH, 25 µg *P. vivax* eIF-5A$^{(dhp)}$, 6 µl 0.1 M DTT, 6 µl 0.1 M NAD, and 240 µl of 125 mM NaH_2PO_4 buffer. In order to investigate the putative inhibitory effects of the Malaria Box compounds of interest, the inhibitors were diluted in DMSO to obtain a 1 mM working solution. The compounds were employed in the enzyme activity in a concentration of 2 µM. All assays were incubated at 37 °C on a shaker for 3 h and the reaction was stopped by freezing at −80 °C. Hypusinated and non-hypusinated eIF-5A was recovered from the assay by employing a two-step size-exclusion chromatography as describe above. The samples were hydrolyzed for 24 h at 110 °C in 6 N HCl before proceeding to GC/MS analysis.

Synthesis of (+)-hypusine

A number of approaches have been reported in the literature for the stereoselective synthesis of hypusine (Tice and Ganem 1983; Bergeron et al. 1993, Jain et al. 2001). Due to the readily available starting materials, a method employing protected lysine and (*S*)-(+)-epichlorohydrin was chosen (Bergeron et al. 1993).

As depicted in Fig. 3, the commercially available *N*-Cbz-L-lysine benzyl ester (**1**) was first converted to *N*-benzyl-*N*-Cbz-L-lysine benzyl ester (**2**) by reductive amination with benzaldehyde employing sodium cyanoborohydride in aqueous solution. *N*-protected derivative (**2**) was subsequently reacted with (*S*)-(+)-epichlorohydrin providing chlorohydrin (**3**), which was then transformed into cyano derivative (**4**) by means of potassium cyanide. In the final step, hydrogenation of the cyano group and hydrogenolysis of protecting groups using platinum oxide as catalyst and hydrogen at atmospheric pressure gave rise to (2*S*, 9*R*)-(+)-hypusine (**5**) in 6 % overall yield. All intermediates and the product were characterized by ^{1}H NMR as well as MS and the spectral data for the substances matched those reported by Bergeron et al. (Bergeron et al. 1993).

The crude product obtained after hydrogenation was purified by preparative reversed phase HPLC with a Phenomenex Aqua 250 × 21.2 mm i.d. column, packed with spherical 10 µm C18 silica using water/acetonitrile (9/1) containing 10 mM of ammonium formate buffer as the mobile phase.

GC/MS analysis

The GC/MS method used to analyze deoxyhypusine and hypusine is a modified version of a previously described

approach (Horak et al. 2014). After transferring 200 µL of the peptide hydrolysates into a glass vial, 125 pmol norvaline was added to the sample as an internal standard. The solvent was removed using a speedvac vacuum concentrator (Thermo Electron Corporation, Savant ISS110, Karlsruhe, Germany).

For esterification of the carboxyl group, 250 µL of a mixture containing deuterated ethanol and acetyl chloride [85/15 (v/v)] was added and the sample was derivatized at 110 °C for 20 min. Afterwards, the derivatization reagent was removed at 110 °C by a gentle steam of nitrogen. For the subsequent derivatization of the amino function, 250 µL of a mixture of trifluoroacetic acid anhydride and trifluoroacetic acid ethyl ester [1:2 (v/v)] was added to the sample and heated at 130 °C for 10 min. The reagent was then removed at room temperature by a gentle steam of nitrogen. An additional derivatization for the hydroxyl group of hypusine was necessary. For this purpose, 100 µL hexamethyldisilazane was added and the sample heated for 15 min at 70 °C. Following the addition of 50 µL of dichloromethane, the solution was transferred to the GC vial and injected.

An Agilent Technologies 7890 A GC-System with MS detector (MS Agilent Technologies 5975 C inert MSD with Triple-Axis) and a DB5-MS capillary column (30 m × 250 µm i.d. × 0.1 µm film thickness) from Agilent (Waldbronn, Germany) was employed. The injection volume was 1 µL and applied in the splitless mode using helium as carrier gas with a flow rate of 1 mL/min. A temperature program was used to maintain a temperature of 50 °C for 0.75 min, then ramping to 75 °C with 50 °C/min and keeping it for 1 min, followed by an increase of the temperature with 6 °C/min to 280 °C with a final hold for 10 min. The chromatogram was acquired by selected ion monitoring (SIM), using for norvaline $m/z = 126$, 168 and 199, for deoxyhypusine $m/z = 126$, 180 and 533, and for hypusine $m/z = 129$, 242 and 606. The sum of the signal intensities of each of the three ions was accumulated and used for quantification of the respective substance.

Two different procedures of processing of the GC/MS data were employed to analyze the samples. The first method, which was previously described (Atemnkeng et al. 2013; Njuguna et al. 2014), leads to a relative quantification of the amino acids in % within a sample by comparing the peak areas of the analytes. For obtaining insight into the absolute inhibition of *P. falciparum* DOHH by the compounds of interest, a method using hypusine (for synthesis as described above) and deoxyhypusine (Kaiser et al. 2012) as standards as well as norvaline (Sigma Aldrich, Munich, Germany) as an internal standard was established. This method allows for quantification of hypusine in the pmol/µl concentration range. Both approaches allow for an expression of inhibition in % following analysis.

Western blot analysis

Two polyclonal antibodies were applied for Western Blot analyses, i.e., IU-88 (Nishiki et al. 2013) and anti-eIF-5A raised against the eIF-5A protein from *P. vivax* (Kerscher et al. 2010). IU-88 is an antibody that specifically differentiates between the modified and unmodified forms of human eIF-5A (Nishiki et al. 2013). This antibody was kindly provided by Dr. B. Maier and Dr. R. G. Mirmira, Department of Medicine, Indiana University School of Medicine, Indianapolis, USA. The anti-eIF-5A antibody was raised against purified eIF-5A protein from *P. vivax* as described previously (Kerscher et al. 2010). After separation of the proteins on 10 % SDS PAGE gels by gel electrophoresis, proteins were transferred onto a nitrocellulose membrane (Bio-Rad, Munich, Germany) employing a semi-dry transfer method according to a modified standard Bio-Rad protocol (Bio-Rad, Munich, Germany). The IU-88 polyclonal primary antibody was diluted 1:500 in PBS buffer with 5 % skim milk and 0.2 % Tween and incubated for 1 h at room temperature. Thereafter, the membrane was washed four times with PBS-buffer containing 0.1 % Tween 20 for 5 min to deplete unbound primary antibody. The secondary dye conjugated anti-IgG antibody IRDye 800 CW was diluted 1:10,000 in PBS, 5 % skim milk and 0.2 % Tween and incubated for 20 min at room temperature. Unbound secondary antibody was washed out with PBS-buffer (0.1 % Tween 20) three times for 5 min and finally pure PBS-buffer for 5 min. Membranes were dried in the dark and subsequently the immunoblot analysis was visualized using a LI-COR Odyssey fluorescence system. For Western Blot analysis with the primary anti-eIF-5A antibody, the antibody was diluted 1:200 in PBS-buffer with 5 % skim milk and 0.2 % Tween.

Results

Target validation of *P. falciparum* DOHH with compounds from the Malaria Box

The previously described 40 most active compounds of the Malaria Box (Avery et al. 2014) were empirically pre-selected for potential iron complexing agents. This approach resulted in three compounds, i.e., the bis-benzimidazole A03 (MMV666023), the naphthyl azobenzimidazole B08 (MMV007384), and a 1,2,5-oxadiazole C03 (MMV665805). These compounds were screened for their potential to suppress hypusine synthesis by *P. falciparum*

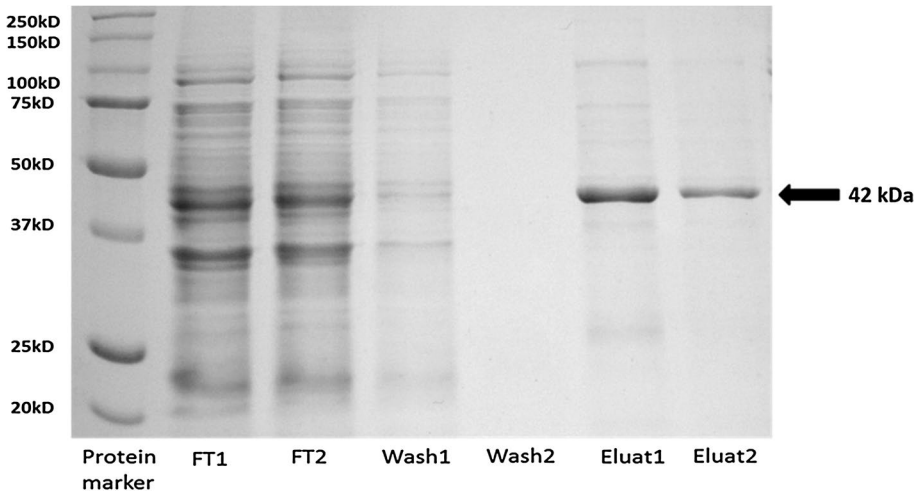

Fig. 4 Expression and purification of *Plasmodium falciparum* DOHH: *P. falciparum* DOHH was purified by Nickel-chelate affinity chromatography. Separation was performed on a 10 % SDS gel, which was stained in blue Coomassie dye. The *lanes* shown are (*left* to *right*) the Precision Plus Protein marker (Bio-Rad, Munich, Germany), Column Flowthrough 1 and 2, Wash fractions 1 and 2 and Eluate fractions 1 and 2. The purified 42 kDa DOHH Protein is marked by the *arrow*

DOHH via complexing the iron ions in the active site. To obtain DOHH for the inhibitor assay, we optimized the expression of *P. falciparum* DOHH in a recombinant *pET-28A* expression vector in *E. coli* BL21 cells and started the subsequent purification of the DOHH protein under native conditions. A soluble protein of 42 kDa size was recovered at 250 mM imidazole concentration in eluate fractions 1 and 2 after nickel chelate affinity chromatography. The estimated size of the yielded protein matches the one of previously expressed *P. falciparum* DOHH protein (Frommholz et al. 2009). The different steps of DOHH protein purification are illustrated in Fig. 4. However, it is evident that the eluate fraction 2 contained DOHH protein of the highest purity. Protein purification yielded between 480 and 520 µg of pure enzyme per 100 mL bacterial culture after purification and rebuffering. Attempts to combine a desalting step with an affinity chromatography purification step failed in a Profinia System (Bio-Rad, Munich, Germany) (Kaiser, unpublished).

The nickel-affinity purified DOHH enzyme and deoxyhypusinated eIF-5A were employed in the activity assay. After incubation, the protein fraction was recovered, and hypusinated and non-hypusinated eIF-5A were separated from DHS enzyme by a two-step size exclusion chromatography step (12). The protein hydrolysates of isolated hypusinated and non-hypusinated eIF-5A and subsequent peptide hydrolysates were used to study the inhibitory activity of three compounds shown in Fig. 2. It is worth mentioning that compound MMV666023 has already been tested in 21 different functional assays against *Mycobacteria, Schistosomes, Plasmodium* and the worm *Onchocerca linealis* while MMV007384 was recently tested in an antiapicoplast and gametocytocidal screening (Bowman et al. 2014). MMV665805 was very recently identified in a screening for compounds disrupting ion homeostasis in the malaria parasite (Lehane et al. 2014).

GC/MS method for hypusine determination

To analyze the hydroxylase activity of *P. falciparum* DOHH after inhibition with 2 µM of each of the compounds, GC/MS analysis was employed to monitor hypusine formation. For this purpose, derivatization of the amino acids in the protein hydrolysate was necessary. Initially, a relative quantification was employed to derive information on the inhibitory activity because a hypusine standard was not available (Atemnkeng et al. 2013; Njuguna et al. 2014). Thus, deoxyhypusine was quantified with external calibration and hypusine was estimated via the peak area ratio assuming an identical detector response factor. Thereby, a relative % DOHH inhibition between 88 and 94 % relative to the positive control without inhibitor could be derived (Fig. 5). Since it was highly uncertain that the detector response is identical for hypusine and deoxyhypusine, a hypusine standard was synthesized. With both hypusine and deoxyhypusine standards in hand, both compounds could be determined with a validated GC–MS assay using absolute quantification.

A slight modification of the derivatization scheme was necessary. Since the secondary alcohol in the hypusine side chain was not derivatized by the double derivatization protocol commonly utilized for amino acid analysis (Horak et al. 2014), an additional derivatization with trimethylsilazane was carried out affording the trimethylsilylether derivative in the side chain. With this optimized derivatization scheme, hypusine and deoxyhypusine could be both detected in the same GC run with a DB-5 ms capillary column. Figure 6a, b shows GC/MS chromatograms of a standard solution of hypusine and deoxyhypusine with 100 pmol and 1.67 pmol on-column, respectively. The corresponding EI MS spectra of the peak at 27.616 and 26.642 min clearly confirm the elution of the target analytes hypusine and deoxyhypusine, respectively (Fig. 7).

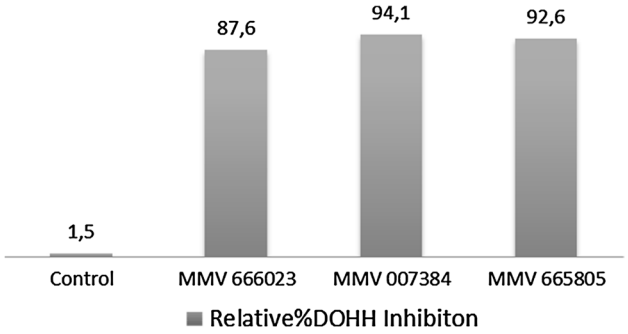

Fig. 5 Inhibitory effects of the Malaria Box compounds on *P. falciparum* DOHH activity obtained by relative GC/MS quantification

The most characteristic fragment ions are indicated by an arrow and were used for quantification by selected ion monitoring (SIM) scan mode.

Thus, for quantification, the accumulated intensities of the ions at $m/z = 126{,}180$ and 533 were used for deoxyhypusine, while for hypusine the m/z values of 129, 242 and 606 were selected. The internal standard norvaline (eluted at 7.611 min) was extracted by accumulation of the signal intensities of the m/z values of 126,168 and 199, using the SIM mode. The method was calibrated in the concentration range of 0.3–5 pmol on-column. For this purpose, stock solutions of norvaline, hypusine and deoxyhypusine were prepared with a concentration of 1 mmol/L each. A dilution series of hypusine and deoxyhypusine was then prepared from the stock solutions to obtain calibrants with always the same concentration of norvaline (125 pmol on column). These mixed standard solutions were then injected into the GC/MS system. A linear response of the peak areas normalized by the peak area of the internal standard was found between 0.3 and 1.7 pmol analyte on column for both hypusine and deoxyhypusine. Corresponding slopes and intercept as well as coefficients of determination are summarized in Table 1. LODs (limits of detection) and LOQs (limits of quantification), were determined based on signal to noise ratios of 3:1 and 9:1, respectively, whereby the noise was measured of the blank signal close to the hypusine and deoxyhypusine peak. LOQs were 0.03 and 1.39 pmol on column for hypusine and deoxyhypusine, respectively (Table 1). Precision and accuracy were determined for a quality control sample containing 0.5 pmol and 1.5 pmol of hypusine and deoxyhypusine, respectively. Accuracies (as determined by % recovery) were good (close to 100 %) with an acceptable precision of 10–15 % (Table 1).

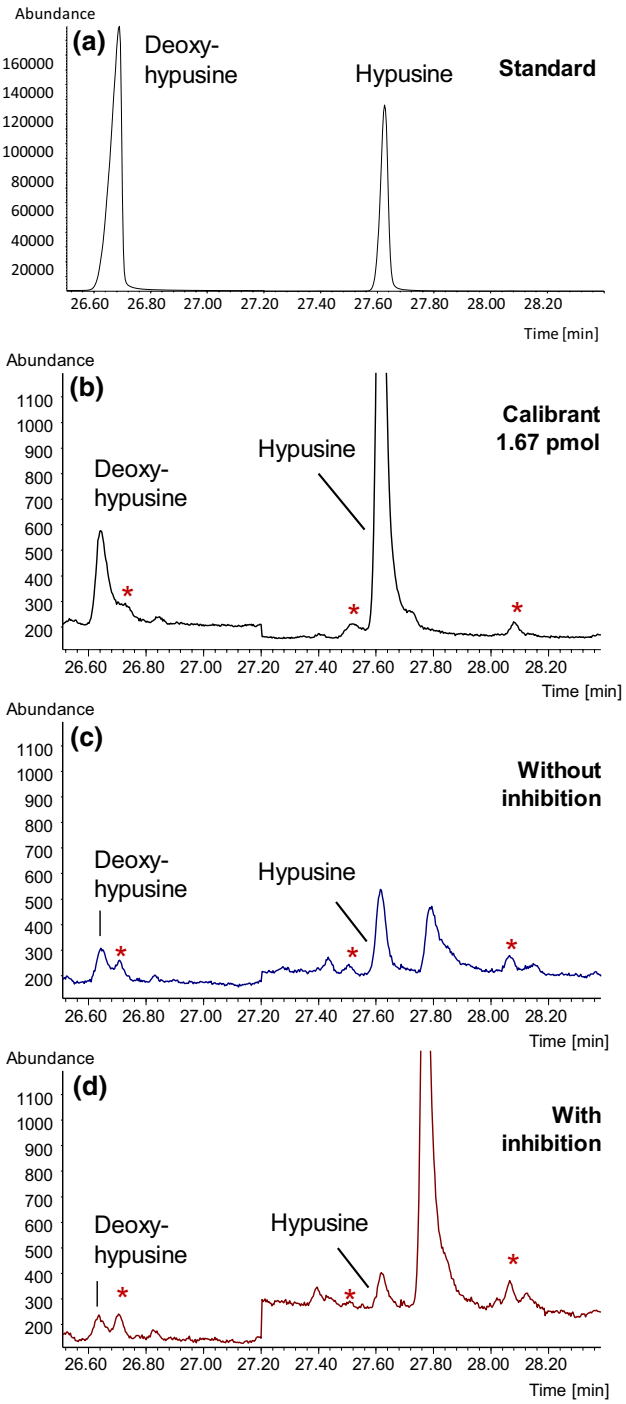

Fig. 6 GC/MS chromatograms showing the relevant part of the chromatogram in which hypusine and deoxyhypusine are eluted. **a** Standard chromatogram with deoxyhypusine and hypusine injected on column, **b** chromatogram of calibrant with 1.67 pmol of deoxyhypusine and hypusine injected on column, **c** sample without inhibitor (positive control), and **d** sample with inhibitor C03 (*asterik* indicates peaks which are also present in the blank)

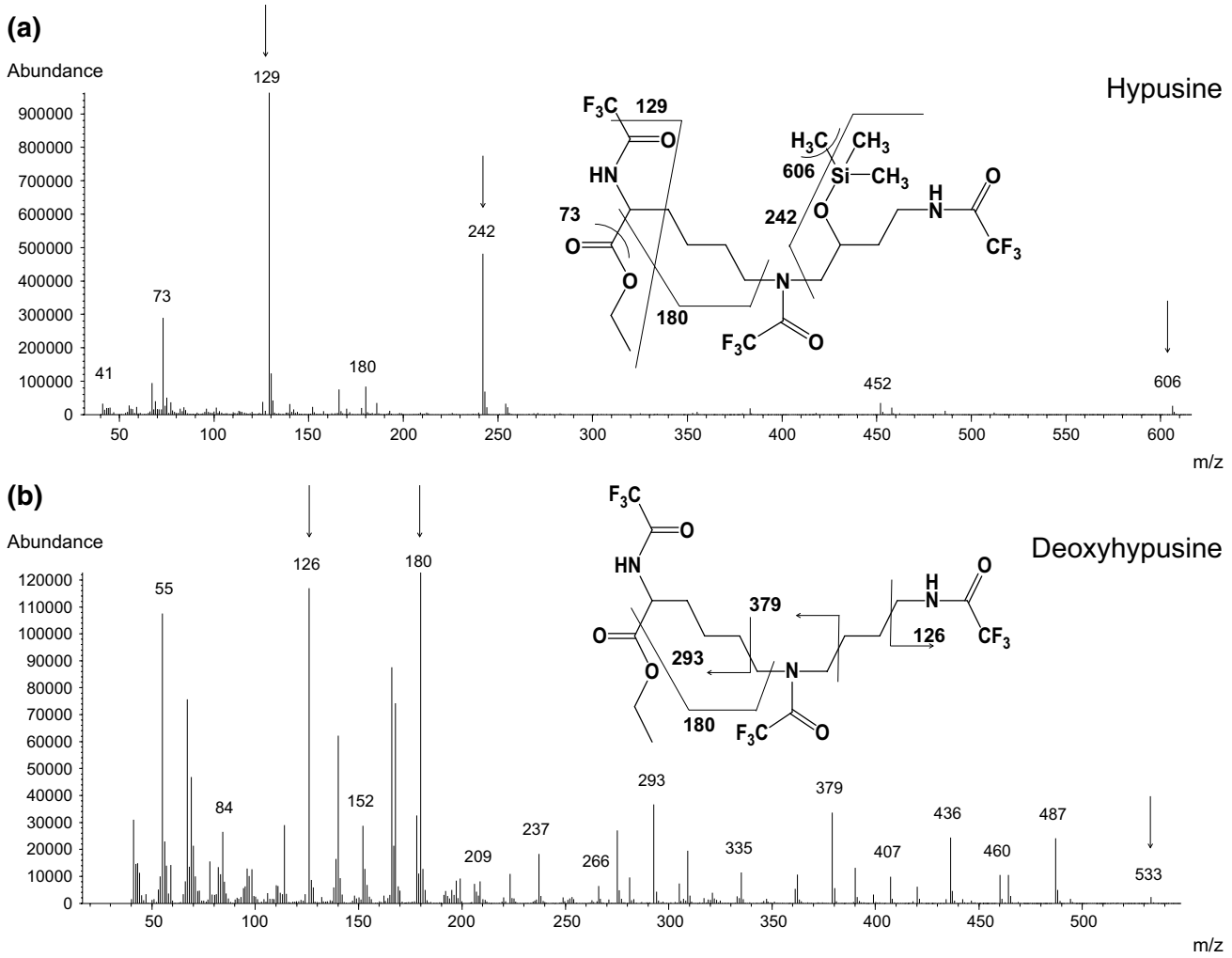

Fig. 7 EI Mass spectra of hypusine (**a**) and deoxyhypusine (**b**) extracted from the peak eluting at 27.616 and 26.638 min, respectively, of the standard shown in chromatogram of Fig. 6b. The most characteristic fragment ions (indicated by *arrows*) are $m/z = 129$, 242 and 606 for hypusine and $m/z = 126$, 180 and 533 for deoxyhypusine

Table 1 Method performance of GC/MS assay and validation data

Amino acid	Retention time (min)	Slope[c]	Intercept[c]	R^{2c}	LOD[a] (pmol)	LOQ[a] (pmol)	Precision RSD (%)	Recovery[b] (%)
Hypusine	26.6	0.3271	−0.0342	0.9981	0.01	0.03	10.6	104
Deoxyhypusine	27.6	0.638	+0.0051	0.9808	0.42	1.39	14.5	103

[a] On column

[b] At a concentration of 0.5 pmol of hypusine and 1.5 pmol of deoxyhypusine on column

[c] Range on column: 0.3–1.7 pmol

Inhibition of DOHH from *P. falciparum* with compounds from the Malaria Box

Next, we performed the DOHH activity assay in the presence of 2 μM of the respective inhibitors A03 (MMV666023), B08 (MMV007384), and C03 (MMV665805). GC/MS analysis of the positive control (Fig. 6c) resulted in a concentration of 31.2 pmol/200 μL hypusine serving as reference value for an incubation without any inhibitory effect. The most potent inhibitor was C03 with 43 % inhibition of parasitic DOHH (Fig. 6d). The benzimidazole-derived inhibitors were slightly less effective with B08 showing 39 % inhibition and A03 showing 36 % inhibition, respectively. These results are summarized in Table 2.

Table 2 Results for quantification of hypusine based on GC/MS

Compound	Absolute GC/MS quantification	
	pmol hypusine/ 200 ul solution	% DOHH inhibition
None	31.24 ± *0.03*	–
MMV666023 (A03)	19.98 ± *0.03*	35.9 ± *0.1*
MMV007384 (B08)	19.10 ± *0.03*	38.8 ± *0.1*
MMV665805 (C03)	17.67 ± *0.03*	43.3 ± *0.1*

Determination of DOHH inhibition was determined by quantification of hypusine based on the established calibration function for hypusine. Results represent the mean value + standard deviation

Standard deviations are given in italics

Two different procedures of processing the GC/MS data were employed to analyze the samples. The first method, which was previously described (Atemnkeng et al. 2013; Njuguna et al. 2014), leads to a relative quantification of the amino acids in % within a sample by comparing the peak areas of the analytes. For obtaining insight into the absolute inhibition of *P. falciparum* DOHH by the compounds of interest, a GC/MS method using hypusine (for synthesis as described above) and deoxyhypusine (Kaiser et al. 2012) as standards as well as norvaline (Sigma-Aldrich, Munich, Germany) as an internal standard was established, which allows quantification of hypusine in the pmol/µL concentration range. Both approaches allow for an expression of inhibition in % following GC/MS analysis.

Predicted iron complexing activity of the antimalarial compounds based on quantum–mechanical calculations

As an indicator for the ability of the three inhibitors to complex ferrous iron ions, the electrostatic surface potential of the compounds was calculated after minimization of the molecules on the B3LYP/6-31G** level of theory. Figure 8a–c show the electrostatic potential of A03, B08 and C03 mapped on their molecular surface. Due to the presence of two or more electron-rich nitrogen and/or oxygen atoms in close proximity arranged in an appropriate geometry, A03 and C03 can be expected to chelate iron ions forming bidentate complexes. In contrast, B08 possesses only a single coordination site. It is known from the Pearson concept of hard and soft acids and bases (HSAB) (Pearson 1963), that iron(II) ions favor binding to aromatic sp^2-hybridized nitrogen atoms as they are found in imidazole or related heterocycles. Consequently, all of the compounds should be capable of potently complexing the ferrous iron found in the core of the plasmodial DOHH enzyme. From the calculations of the electrostatic surface potential, it is obvious that compound C03 can be expected to possess the strongest iron(II)-complexing properties, which is in accordance with the biological data from Table 2. As seen in the 3-dimensional structure (Fig. 8a), the oxadiazole N2-nitrogen atom and the amide carbonyl group arrange in a coplanar fashion offering two strongly negative polarized coordination sites to chelate iron. Compound A03 (Fig. 8c) also fulfills the geometric requirements for iron chelation. However, the electron density is mainly located on the benzimidazole N3-atom, suggesting that the lone pair of the diazo nitrogen atom, possessing a comparably low negative charge density, only weakly contributes to iron coordination. Therefore, a lower overall affinity towards iron ions can be expected when compared to C03. Interestingly, the biological data show that compound B08 is a marginally more potent inhibitor in comparison to A03, despite the lack of a second iron coordination site (Fig. 8b), which might be exploited for forming a chelate complex. These findings suggest that bulky A03 does not properly fit the binding site of the enzyme leading to decreased affinity, while the linear compound B08 might compensate its weaker iron-complexing properties by a better fit to the enzymes active site. However, the latter hypothesis is highly speculative and X-ray crystallographic data would be beneficial for gaining further insight into the binding modes of those compounds, allowing for a structure-based optimization.

Discussion

Three diverse chemotypes have been identified from the Malaria Box, i.e., an azonapthyl benzimidazole (A03), a bis-benzimidazole (B08), and a 1,2,5-oxadiazole (C03) to inhibit the second enzyme of the hypusine pathway, the deoxyhypusine hydroxylase. Due to characteristic structural features of those compounds, we assume that iron complexation is the key mechanism causing the inhibitory activity. The benzimidazole MMV007384 (B08) is a probe-like compound, which was originally characterized in a screening for its gametocytocidal and antiapicoplast activity (Bowman et al. 2014). However, the compound exhibits an IC_{50} of 870 ± 180 nM in gametocytes of the strain NF54 in vitro. By contrast, epoximicin functions as a positive control against gametocytes with an IC_{50} of 3.8 ± 0.2 nM. This result demonstrates that the drug is not a typical gametocytocidal compound but might display a more significant effect in vivo. Moreover, MMV007384 (B08) has only a moderate activity against the asexual, erythrocytic blood stages of the chloroquine-sensitive strain NF54 resulting in an IC_{50} of 100 ± 7 nM and an IC_{50} of 190 ± 20 nM against the Dd2 strain. In summary, the benzimidazole MMV007384 exerted an inhibitory effect on recombinant deoxyhypusine hydroxylase in vitro presumably due to its iron complexation properties via one of its electron-rich benzimidazole rings, which is well suited for

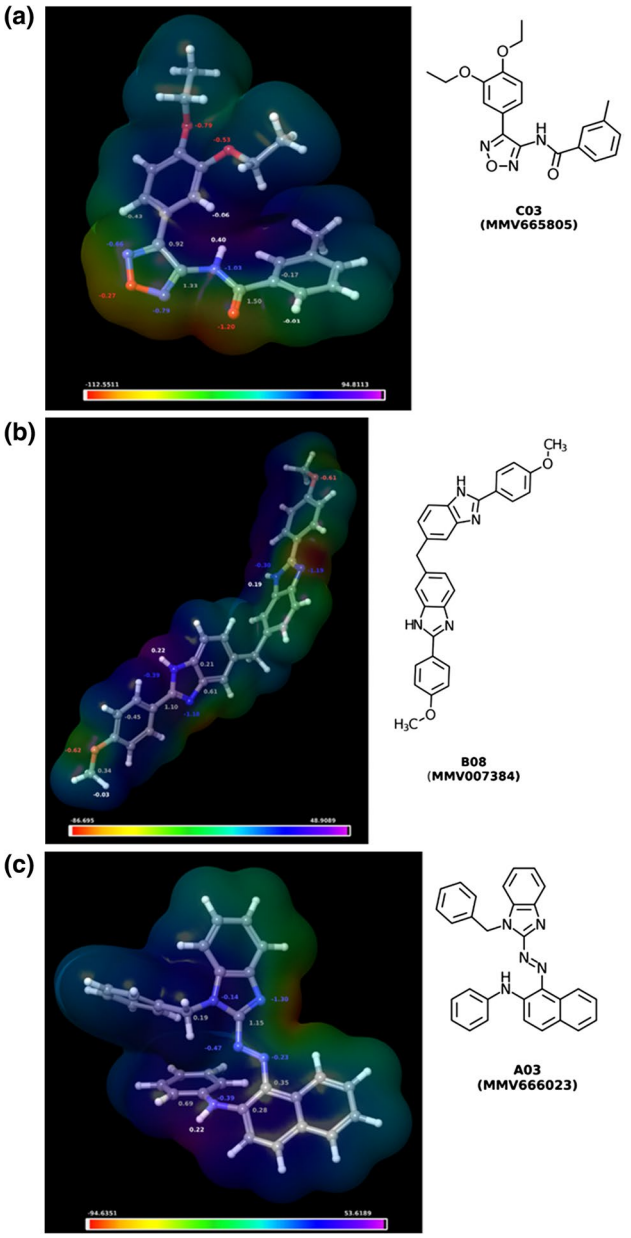

Fig. 8 Molecular electrostatic potential of compounds C03, B08 and A03 and partial charges for selected atoms. The electrostatic potential is mapped on the molecular surface at an isovalue of 0.001 electrons/Bohr^3. Negatively polarized areas are shown in *red*, while areas with a positive polarization are indicated by a *blue-shift*. **a** A potential iron chelating site in C03 is located between the oxadiazole N2-atom and the neighboring amide carbonyl function. **b** A potential iron coordination site in B08 is located on both of the benzimidazole N3-atoms. Due to the geometry of the molecule, it is unlikely that the nitrogen lone-pairs of both benzimidazole residues can coordinate a single ion. **c** A potential iron chelating site in A03 is located between the benzimidazole N3-atom and the second diazo nitrogen atom. The later features a lower electron density compared to the chelating motif in C03 suggesting a lower affinity towards the iron(II) center. Calculations were performed at the B3LYP/6-31G** level of theory using Jaguar (Schroedinger Small Molecule Drug Discovery Suite, Release 2014-3) (color figure online)

the complexation of ferrous iron according to the Pearson HSAB concept. Compound MMV665805 (C03) was previously tested in a screening that disrupts ion homeostasis in the malaria parasite (Lehane et al. 2014). It was characterized as one of four chemotypes resulting in multiple hits in Na^+ and pH assays. Compounds with a spiroindolone structure resulted in Na dependent ATPase activity in parasite-erythrocyte membrane preparations. Therefore, this compound serves as an inhibitor of the PfATP4 protein, which is an efflux pump that expels Na^+ from the parasite in exchange with H^+. Compound MMV665805 (C03) exhibited the best inhibitory property on DOHH in the activity assay. The superior inhibitory potency compared to B08 and C03 might be attributed to its stronger iron-complexation capacity. This is in accordance with quantum–mechanical calculations, highlighting the high electron density located on the oxadiazole N2 lone-pair and the neighboring amide carbonyl group, which are arranged in a favorable geometry for bidentate coordination. Hitherto, there is no published information about the mode of action of compound MMV666023 (A03). However, the compound has been investigated in a variety of biological assays against *Mycobacteria, Schistosomes, Plasmodium and Onchocerca* but without significant activity except for *Plasmodium*.

For a high-throughput screening (HTS) of inhibitors for each of the enzymes of the hypusine pathway a rapid, robust and precise analytical assay has to be established. Herein we demonstrated that besides the portfolio of proteomic tools (von Koschitzky and Kaiser 2013) GC/MS is also a valid technique to quantify deoxyhypusine and hypusine metabolites. However, the screening of a compound library needs further simplification and automatization in a microtiter plate scale (Derbyshire et al. 2012). In this context, direct antibodies against deoxyhypusine and hypusine would be of significant advantage. Recently, Mirmira et al. reported results about a polyclonal antibody IU-88 that specifically recognizes the hypusinated form of eIF-5A (Nishiki et al. 2013). However, the antibody was unable to distinguish between the deoxyhypusinated and hypusinated form of eIF-5A for unknown reasons (Nishiki et al. 2013). The fact that the antibody IU-88 recognizes the hypusinated form of human eIF-5A prompted us to investigate whether it is able to recognize the deoxyhypusinated form of modified plasmodial eIF-5A (Fig. 9). In a first set of experiments the hypusine specific human antibody IU-88 detected a clear signal with a molecular size of 44 kDa in a whole cell lysate of 293T cells coexpressing a GFP-fusion protein of human eIF-5A and a GFP-DHS fusion protein-encoding vector (Fig. 9a, lanel). However, no signal was obtained when the antibody IU-88 was used to detect the deoxyhypusinated form of Plasmodium eIF-5A (Fig. 9a, lane 2) in a typical DHS assay applying recombinant DHS protein from human and plasmodial

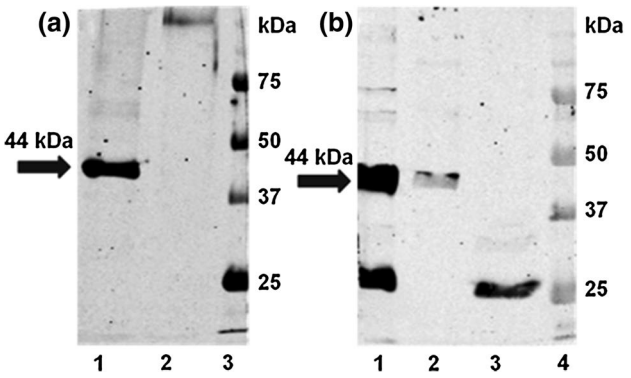

Fig. 9 Western Blot analysis with IU-88 and plasmodial anti-eIF-5A polyclonal antibodies detecting hypusinated forms of eIF-5A from human and Plasmodium. Signal detection was visualized using a LI-COR Odyssey fluorescence system. In Blot (**a**) a specific anti-hypusine antibody IU-88 was applied. *Lane* 1: Whole cell lysate of 293T cells transfected with GFP-tagged eIF-5A and a GFP-DHS encoding fusion protein-encoding vector, *lane 2*: *P. vivax* eIF-5A incubated with human DHS and *lane 3*: Precision Plus Marker (Bio-Rad, Munich, Germany). In Blot (**b**) a plasmodial, polyclonal anti-EIF-5A antibody was used for detection. *Lane 1*: purified GST-tagged human eIF-5A (GST column eluate), *lane 2*: Whole cell lysate of 293T cells transfected with GFP-tagged eIF-5A and DHS, *lane3*: *P. vivax* eIF-5A incubated with human DHS and *lane 4*: Precision Plus Marker

eIF-5A protein. By contrast, DHS activity could be detected by GC/MS for the presence of deoxyhypusine (data not shown). Crossreactivity could be demonstrated when the plasmodial, polyclonal anti-eIF-5A antibody was applied to detect the GST-tagged human eIF-5A protein (Fig. 9b, lane 1). Plasmodial anti-eIF-5A antibody clearly detected the purified eIF-5A protein in control panel 3 (Fig. 9b) with the expected size of 22 kDa. The polyclonal IU-88 anti-human eIF-5A antibody was raised against the peptide C-Ahx-STSKTG-hypusine-HGHAKV- containing two motifs surrounding the hypusine loop. However, the second motif surrounding the hypusine residue in human differs with respect to the plasmodial eIF-5A protein. In the human eIF-5A protein, the second peptide motif consists of the terminal amino acid valine instead of alanine present in plasmodial eIF-5A. In sum, this amino acid difference might cause the specificity of the antibody recognizing the hypusine epitope of human eIF-5A and fails to detect the plasmodial orthologue. Moreover, differences in the vicinity of the second motif surrounding the hypusine loop might contribute to a different folding of plasmodial EIF-5A and in consequence to a different exposure of the hypusine residue, which prevents the recognition of plasmodial eIF-5A hypusine epitope.

In this study we have improved the quantification of the hypusine metabolites for target evaluation of DOHH from *P. falciparum* by GC/MS analysis subsequent to triple derivatization (esterification of carboxyl group, trifluoroacetylation of primary and secondary amino groups, and trimethylsilylation of secondary hydroxyl in the side chain of hypusine). We have demonstrated the inhibitory properties of three compounds from the Malaria Box, which are probably related to their ability to coordinate the ferrous ions found at the active site of plasmodial DOHH. Absolute quantification was improved using the SIM mode accumulating the signals for three characteristic ions of each hypusine and deoxyhypusine. The limit of detection (LOD) for hypusine was 0.01 pmol and for deoxyhypusine it was 0.42 pmol. Moreover, the precision and accuracy of the method was increased by the application of an internal standard like norvaline. Hitherto, this method is only suitable for a target validation but might be suitable for a HTS once the activity assay is scaled down to a microtiter plate format. Recent results demonstrated the successful identification of non-hypusinated and hypusinated eIF-5A in SIM mode by GC/MS in the plant *Arabidopsis thaliana* after induction with abscisic acid (Belda-Palazon et al. 2014). However, hypusine metabolites were not quantified.

In parallel, a relative quantification of hypusine inhibition was performed by comparison of the relative peak areas of deoxyhypusine and hypusine (Fig. 5). Using this approach, MMV007384 and MMV665805 exhibited an efficacy of 94.1 and 92.6 % inhibition of *P. falciparum* DOHH, while both quantification methods demonstrated lowest inhibition for the compound MMV666023 suggesting that absolute quantification is necessary to evaluate target specific inhibition of plasmodial DOHH.

Our results clearly demonstrate that the effect of DOHH inhibition can vary between compounds having a benzimidazole structure as a part of the scaffold. In this context substituents of the benzimidazol structure seem to be responsible for the efficacy. In sum, crystallization experiments of Plasmodium DOHH will facilitate further target evaluation.

Acknowledgments This work was supported by Grants from the DAAD (Project-ID 57068252) and Heinz und Gertie Fischer Stiftung to AK. The authors acknowledge receipt of the antibody IU-88 from Dr. RG Mirmira, Department of Medicine, Indiana University School of Medicine, Indianapolis, USA.

Conflict of interest The authors declare that they have no competing interest.

References

Andrus L, Szabo P, Grady RW, Hanauske AR, Huima-Byron T, Slowinska B, Zagulska S, Hanauske-Abel HM (1998) Antiretroviral effects of deoxyhypusyl hydroxylase inhibitors: a hypusine-dependent host cell mechanism for replication of human immunodeficiency virus type 1 (HIV-1). Biochem Pharmacol 55:1807–1818

Assaraf YG, Golenser J, Spira DT, Bachrach U (1984) Polyamine levels and the activity of their biosynthetic enzymes in human erythrocytes infected with the malaria parasite, *Plasmodium falciparum*. Biochem J 222:815–819

Atemnkeng VA, Pink M, Schmitz-Spanke S, Wu XJ, Dong LL, Zhao KH, May C, Laufer S, Langer B, Kaiser A (2013) Deoxyhypusine

hydroxylase from Plasmodium vivax, the neglected human malaria parasite: molecular cloning, expression and specific inhibition by the 5-LOX inhibitor zileuton. PLoS One 8:e58318

Avery VM, Bashyam S, Burrows JN, Duffy S, Papadatos G, Puthukkuti S, Sambandan Y, Singh S, Spangenberg T, Waterson D, Willis P (2014) Screening and hit evaluation of a chemical library against blood-stage *Plasmodium falciparum*. Malar J 13:190-2875-13-190

Baird JK, Hoffman SL (2004) Primaquine therapy for malaria. Clin Infect Dis 39:1336–1345

Belda-Palazon B, Nohales MA, Rambla JL, Acena JL, Delgado O, Fustero S, Martinez MC, Granell A, Carbonell J, Ferrando A (2014) Biochemical quantitation of the eIF5A hypusination in Arabidopsis thaliana uncovers ABA-dependent regulation. Front Plant Sci 5:202

Bergeron RJ, Xia MX, Phanstiel O IV (1993) Total syntheses of ()-hypusine and its (2S, 9S)-diastereomer. J Org Chem 58:6804–6806

Birkholtz LM, Williams M, Niemand J, Louw AI, Persson L, Heby O (2011) Polyamine homoeostasis as a drug target in pathogenic protozoa: peculiarities and possibilities. Biochem J 438:229–244

Bowman JD, Merino EF, Brooks CF, Striepen B, Carlier PR, Cassera MB (2014) Antiapicoplast and gametocytocidal screening to identify the mechanisms of action of compounds within the malaria box. Antimicrob Agents Chemother 58:811–819

Chawla B, Kumar RR, Tyagi N, Subramanian G, Srinivasan N, Park MH, Madhubala R (2012) A unique modification of the eukaryotic initiation factor 5A shows the presence of the complete hypusine pathway in Leishmania donovani. PLoS One 7:e33138

Clement PM, Hanauske-Abel HM, Wolff EC, Kleinman HK, Park MH (2002) The antifungal drug ciclopirox inhibits deoxyhypusine and proline hydroxylation, endothelial cell growth and angiogenesis in vitro. Int J Cancer 100:491–498

Derbyshire ER, Mazitschek R, Clardy J (2012) Characterization of Plasmodium liver stage inhibition by halofuginone. Chem Med Chem 7:844–849

Frey AG, Nandal A, Park JH, Smith PM, Yabe T, Ryu MS, Ghosh MC, Lee J, Rouault TA, Park MH, Philpott CC (2014) Iron chaperones PCBP1 and PCBP2 mediate the metallation of the dinuclear iron enzyme deoxyhypusine hydroxylase. Proc Natl Acad Sci USA 111:8031–8036

Frommholz D, Kusch P, Blavid R, Scheer H, Tu JM, Marcus K, Zhao KH, Atemnkeng V, Marciniak J, Kaiser AE (2009) Completing the hypusine pathway in Plasmodium. FEBS J 276:5881–5891

Gamo FJ, Sanz LM, Vidal J, de Cozar C, Alvarez E, Lavandera JL, Vanderwall DE, Green DV, Kumar V, Hasan S, Brown JR, Peishoff CE, Cardon LR, Garcia-Bustos JF (2010) Thousands of chemical starting points for antimalarial lead identification. Nature 465:305–310

Guiguemde WA, Shelat AA, Bouck D, Duffy S, Crowther GJ, Davis PH, Smithson DC, Connelly M, Clark J, Zhu F, Jimenez-Diaz MB, Martinez MS, Wilson EB, Tripathi AK, Gut J, Sharlow ER, Bathurst I, El Mazouni F, Fowble JW, Forquer I, McGinley PL, Castro S, Angulo-Barturen I, Ferrer S, Rosenthal PJ, Derisi JL, Sullivan DJ, Lazo JS, Roos DS, Riscoe MK, Phillips MA, Rathod PK, Van Voorhis WC, Avery VM, Guy RK (2010) Chemical genetics of Plasmodium falciparum. Nature 465:311–315

Horak J, Gerhardt H, Theiner J, Lindner W (2014) Correlation between amino acid racemization and processing conditions for various wheat products, oil seed press cakes and lignin samples. Food Bioprod Process 92:355–368

Jain RP, Albrecht BK, DeMong DE, Williams RM (2001) Asymmetric synthesis of ()-hypusine. Org Lett 3:4287–4289

Kaiser A (2012) Translational control of eIF5A in various diseases. Amino Acids 42:679–684

Kaiser A, Hammels I, Gottwald A, Nassar M, Zaghloul MS, Motaal BA, Hauber J, Hoerauf A (2007) Modification of eukaryotic initiation factor 5A from Plasmodium vivax by a truncated deoxyhypusine synthase from Plasmodium falciparum: an enzyme with dual enzymatic properties. Bioorg Med Chem 15:6200–6207

Kaiser A, Khomutov AR, Simonian A, Agostinelli E (2012) A rapid and robust assay for the determination of the amino acid hypusine as a possible biomarker for a high-throughput screening of antimalarials and for the diagnosis and therapy of different diseases. Amino Acids 42:1651–1659

Kang KR, Kim YS, Wolff EC, Park MH (2007) Specificity of the deoxyhypusine hydroxylase-eukaryotic translation initiation factor (eIF5A) interaction: identification of amino acid residues of the enzyme required for binding of its substrate, deoxyhypusine-containing eIF5A. J Biol Chem 282:8300–8308

Kerscher B, Nzukou E, Kaiser A (2010) Assessment of deoxyhypusine hydroxylase as a putative, novel drug target. Amino Acids 38:471–477

Krotoski WA (1989) The hypnozoite and malarial relapse. Prog Clin Parasitol 1:1–19

Lehane AM, Ridgway MC, Baker E, Kirk K (2014) Diverse chemotypes disrupt ion homeostasis in the malaria parasite. Mol Microbiol 94:327–339

Milord F, Pepin J, Loko L, Ethier L, Mpia B (1992) Efficacy and toxicity of eflornithine for treatment of Trypanosoma brucei gambiense sleeping sickness. Lancet 340:652–655

Nishiki Y, Farb TB, Friedrich J, Bokvist K, Mirmira RG, Maier B (2013) Characterization of a novel polyclonal anti-hypusine antibody. SpringerPlus 2:1–5

Njuguna JT, von Koschitzky I, Gerhardt H, Lammerhofer M, Choucry A, Pink M, Schmitz-Spahnke S, Bakheit MA, Strube C, Kaiser A (2014) Target evaluation of deoxyhypusine synthase from Theileria parva the neglected animal parasite and its relationship to *Plasmodium*. Bioorg Med Chem 22:4338–4346

Park JH, Aravind L, Wolff EC, Kaevel J, Kim YS, Park MH (2006) Molecular cloning, expression, and structural prediction of deoxyhypusine hydroxylase: a HEAT-repeat-containing metalloenzyme. Proc Natl Acad Sci USA 103:51–56

Pearson RG (1963) Hard and soft acids and bases. J Am Chem Soc 85:3533–3539

Saeftel M, Sarite RS, Njuguna T, Holzgrabe U, Ulmer D, Hoerauf A, Kaiser A (2006) Piperidones with activity against Plasmodium falciparum. Parasitol Res 99:281–286

Spangenberg T, Burrows JN, Kowalczyk P, McDonald S, Wells TN, Willis P (2013) The open access malaria box: a drug discovery catalyst for neglected diseases. PLoS One 8:e62906

Teng R, Junankar PR, Bubb WA, Rae C, Mercier P, Kirk K (2009) Metabolite profiling of the intraerythrocytic malaria parasite Plasmodium falciparum by (1)H NMR spectroscopy. NMR Biomed 22:292–302

Thompson GM, Cano VS, Valentini SR (2003) Mapping eIF5A binding sites for Dys1 and Lia1: in vivo evidence for regulation of eIF5A hypusination. FEBS Lett 555:464–468

Tice CM, Ganem B (1983) Chemistry of naturally occurring polyamines. 8. Total synthesis of (+)-hypusine. J Org Chem 48:5048–5050

Umland TC, Wolff EC, Park MH, Davies DR (2004) A new crystal structure of deoxyhypusine synthase reveals the configuration of the active enzyme and of an enzyme.NAD.inhibitor ternary complex. J Biol Chem 279:28697–28705

von Koschitzky I, Kaiser A (2013) Chemical profiling of deoxyhypusine hydroxylase inhibitors for antimalarial therapy. Amino Acids 45:1047–1053

Vu VV, Emerson JP, Martinho M, Kim YS, Munck E, Park MH, Que L Jr (2009) Human deoxyhypusine hydroxylase, an enzyme involved in regulating cell growth, activates O2 with a nonheme diiron center. Proc Natl Acad Sci USA 106:14814–14819